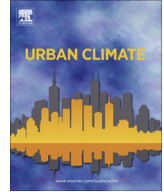




ELSEVIER

Contents lists available at ScienceDirect

Urban Climate

journal homepage: www.elsevier.com/locate/uclim

Influence of virtual changes in building configurations of a real street canyon on the dispersion of PM₁₀

J. Garcia^{a,*}, R. Cerdeira^a, N. Tavares^a, L.M.R. Coelho^a, Prashant Kumar^{b,c}, M.G. Carvalho^{d,e}

^a Escola Superior de Tecnologia de Setúbal, Instituto Politécnico (ESTSetubal-IPS), Setúbal, Portugal

^b Department of Civil and Environmental Engineering, Faculty of Engineering and Physical Science (FEPS), University of Surrey, GU2 7XH, United Kingdom

^c Environmental Flow (EnFlo) Research Centre, FEPS, University of Surrey, GU2 7XH, United Kingdom

^d Instituto Superior Técnico (IST), Lisbon, Portugal

^e European Parliament, Brussels, Belgium

ARTICLE INFO

Article history:

Received 20 November 2012

Revised 22 July 2013

Accepted 13 August 2013

Available online xxxx

Keywords:

PM₁₀ dispersion

CFD code FLUENT

Barreiro street canyon

Real and virtual building configurations,

Traffic emissions

ABSTRACT

Four geometrical configurations of a real street canyon in Barreiro city (Portugal) are considered to study their influence on the dispersion of PM₁₀. These configurations include actual architectural layout of the street (Option 1), and three virtual cases (Options 1–3). Option 2 includes the modification of real geometry by including 4 m gaps between the buildings situated on the southern part of the street canyon. Option 3 considers 6 m gaps between buildings as opposed to 4 m gaps in Option 2. Option 4 assumes the same height for all buildings on the southern part of the street canyon, with no gaps between buildings. Computational fluid dynamics code (CFD), FLUENT, is used to simulate the detailed flow and turbulence characteristics in three-dimensional domain of chosen street canyon, together with the PM₁₀ dispersion for both the summer and winter seasons. The modelled PM₁₀ concentrations were then compared with the measured data at seven different locations in the street canyon. Our results indicate up to 23% lower PM₁₀ concentrations at 1.5 m above the road level during the along-canyon wind direction due to the channelling of flow, compared with those observed during the cross-canyon wind direction. Detailed inspection of the results obtained from the Options 1–3 indicated that the spacing between the buildings tend to increase particle dilution during the cross-canyon winds,

* Corresponding author. Tel.: +351 936262081.

E-mail address: joao.garcia@estsetubal.ips.pt (J. Garcia).

resulting in up to 20, and 22% reduced concentrations for options 2, and 3 respectively, compared with the actual configuration (Option 1). The largest improvement (~7%) in the PM₁₀ concentrations was given by Option 2, while other options showed modest changes. Possible reasons for these changes under varying meteorological conditions are explained in the context of changing building configurations and their implications in city planning.

© 2013 Elsevier Ltd. All rights reserved.

1. Introduction

Planning of urban buildings is important because of its influence on the indoor and outdoor air quality, public health, and sustainable development (EEA, 2011; Kumar and Morawska, 2013). In particular, air quality in urban areas is getting attention, worldwide, due to its adverse impact on the health of city dwellers (Kumar et al., 2011a). In the range of air pollutants, particular attention has been paid to the particulate matter with less than 10 and 2.5 µm in diameter (i.e., PM₁₀ and PM_{2.5}, respectively) (Martins et al., 2009; Amorim et al., 2010; Heal et al., 2012) and more recently to airborne nanoparticles (Kumar et al., 2010, 2011b). Street canyons are considered as a hot spots where exposure levels can be very high due to the build-up of pollutant concentrations as a result of limited dispersion (Britter and Hanna, 2003; Kumar et al., 2008). Numerous epidemiological studies have focused on the PM₁₀ and PM_{2.5} exposure and there are a certain evidences that short term exposure to high concentrations of PM₁₀ can aggravate pulmonary diseases and influence paediatric asthma (Garcia et al., 2010). Likewise, long term exposure to high concentrations on PM₁₀ may increase the risk of cardiovascular and pulmonary disease (WHO, 2004). Topography and urban obstructions such as buildings and other construction influence the atmospheric flow greatly (Britter and Hanna, 2003) and consequently the dispersion of pollutants arising from the vehicle exhausts (Kumar et al., 2011b). Pollutants in street canyons cannot be carried away by the wind easily since the buildings act as a barrier. This results in trapping of pollutants within the canyons (De Paul and Sheih, 1986) and raising their concentrations to high levels (Zhou and Levy, 2008). For instance, a recent study by Wang and Mu (2010) studied the effect of building geometries in street canyons. They found that emissions from intensive traffic flows can raise the pollutant concentrations considerably, depending on the street canyon configuration and the type of flow regimes inside the canyon. Therefore, it is important from the decision makers' point of view to be acquainted with the influence of building density and geometry on the extent of air quality deterioration in urban street canyons.

With the improvement in computational power, dispersion modelling tools such as the computational fluid dynamics (CFD) are particularly useful for simulating the detailed wind and dispersion fields in urban areas that have complex building geometries. The use of CFD tools is complex and resource intensive, but these also provide an opportunity to simulate the complex effect of meteorology and building geometries (e.g. orientation and intensity). Despite the complexity of governing equations (Mochida et al., 2011), the continuous development of powerful numerical codes and implausible increases in hardware performances have made the CFD simulations attractive for complex urban geometries. Numerical simulations have been found to predict the flow and dispersion in urban street canyons fairly well (Sagrado et al., 2002). Vardoulakis et al. (2003) reviewed a number of air quality models for street canyons, including operational, Gaussian plume and CFD models. Their review reports that microscale models such as Microscale MOdel, MIMO (Ehrhard et al., 2000) and mesoscale model MEsokaliges TRAnsport und Stroemungsmodell, METRAS (Schlunzen et al., 1996) are especially designed for street canyon applications. Considering the air quality in roadside environments, the review concluded that CFD has the advantage to reproduce the flow and concentration fields with a reasonable accuracy within urban canyons of any configuration, if the right input data and boundary conditions are supplied. Moreover, field measurements are equally important to complement and validate the modelled CFD results.

Latter, [Holmes and Morawska \(2006\)](#) reviewed various dispersion models (Box, Gaussian, Lagrangian, Eulerian) that are applied to both inert and reactive particles. They reported that the majority of commercial dispersion models do not make any specific treatment of particle dynamics and limit the calculations to particle mass concentrations (PMC). Also was highlighted that the comprehensive performance evaluation of many dispersion models remains an issue due the lack of required measurement data. A number of studies have also compared the CFD simulated results with the measured data, showing under/over prediction of modelled PMCs and attributing these differences in results to the uncertainty in input data ([Pospisil and Jicha, 2008](#); [Santiago and Martín, 2008](#); [Nikolova et al., 2011](#)). For example, [Kumar et al. \(2009\)](#) studied the dispersion of inert nanoparticles in an urban street canyons using a CFD code FLUENT on a simplified canyon geometry, the Operational Street Pollution Model (OSPM) and the modified Box model. The modelled concentrations compared well (between a factor of 2 and 3) with the measured concentrations, suggesting that even a simplified approach can predict the concentrations as well as more complex models if the model inputs are chosen carefully.

In order to carry out parametric studies under different geometrical configurations and wind directions, an operational street canyon in Barreiro city (Portugal) is chosen together with the other three virtual scenarios that reflect modifications in real street canyons (see Section 2.1). The CFD code, FLUENT, is used on three-dimensional site geometry to simulate the influence of the fluid flow on PM₁₀ concentrations in the street canyon; the modeled results are then compared with measured PM₁₀ concentrations. The approach allowed studying the influence of different building configuration, comparison of results obtained in virtual geometries with the actual configuration, and identifying the specific hot spots. The key objectives of this work are to identify the most favourable street configuration for pollutant dispersion, particularly PM₁₀, in different geometrical configurations and meteorological conditions. The findings can assist urban planners to propose environmental friendly design of new housing projects, favouring better air quality.

2. Methodology

2.1. Site description

The studied site, Avenida do Bocage street in Barreiro city, is about 40 km south of Lisbon ([Fig. 1](#)). Barreiro is a relatively small city with about 34 km² surface area and 80,000 inhabitants. Several industrial units such as the combined heat and oil fired power stations, chemical industrial complex, and acrylic fibres factory are near the city centre. Typical city traffic involves buses, heavy duty vehicles (HDVs), light duty vehicles (LDVs; including cars and taxis), and motorcycles. Ground surface of Barreiro is flat and the highest ground level point of the city is at ~10 m above the sea level. This street is an important road – this connects the city centre of Barreiro with a main motorway to the capital of Portugal, Lisbon. The street is ~263 m long and has a width of ~20 m between the both sides of buildings. Heights of the buildings on both side of the street vary between 7 and 39 m. As shown in

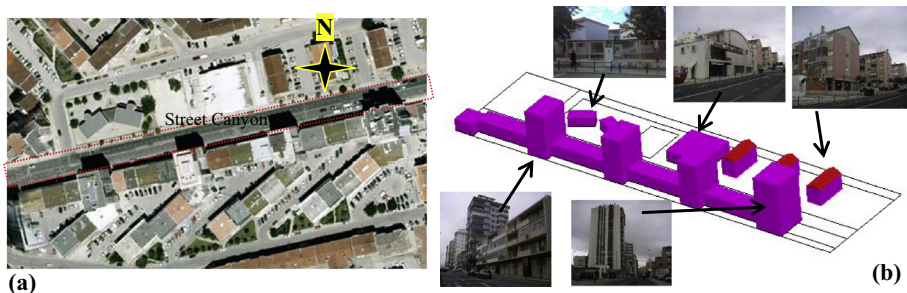


Fig. 1. Schematic diagram of studied street canyon, Avenida do Bocage, showing: (a) aerial view of the street and its orientation, and (b) various snapshots of the canyon along with an idealised computational domain of the entire canyon.

Fig. 1a, the street canyon runs approximately between east and west directions. A sample study was conducted for counting traffic volumes during the PM_{10} measurement campaigns (see Section 2.5). A total of 3794 veh h^{-1} was counted. These included LDVs, HDVs, buses, cars and motorcycles as 95.8%, 1.6%, 2.0% and 0.6% of total vehicles, respectively.

2.2. THE CFD model, FLUENT

The CFD model, Ansys FLUENT 12.0, was used to simulate flow and dispersion of PM_{10} in the selected street canyon. This multi-purpose commercial CFD tool has been widely used for this kind of application and comparison with their results with other dispersion models (Di Sabatino et al., 2008) or wind tunnel measurements (Awasthi and Chaudhry, 2009). The studied domain considered a safety distance to avoid interference of flow between the buildings and both the inlet and outlet domain boundaries. This safety distance was $5H$ (where H is the average height of buildings) from the domain inlet to the buildings location, $15H$ from buildings location to the outlet, and $4H$ from top of buildings (COST, 2007). The simulations were carried out for a total of four wind directions; one of which (West) represents the predominant wind directions for the studied area (see Section 2.5).

The simplified computational domain for the chosen street canyon has length, breadth and height as 715, 300 and 150 m, respectively, for the westerly and easterly wind directions (see Fig. 2).

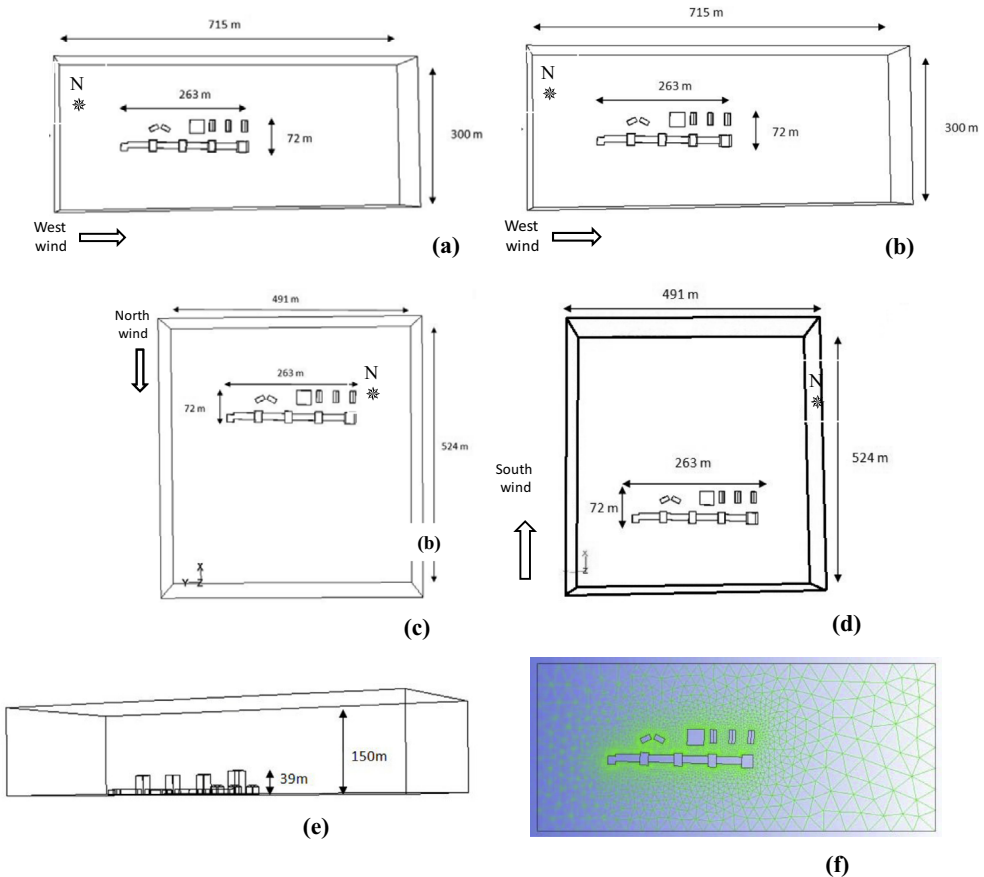


Fig. 2. Schematic diagram showing (a) top plan, for wind from the west direction, (b) top plan for east direction, (c) top plan for north direction, (d) top plan for south direction, (e) side view of the domain, and (f) mesh resolution around buildings.

A tetrahedral unstructured grid was used for the spatial discretisation of the computational domain, which was refined near the buildings. For the construction of the grid Ansys Workbench software (Ansys, 2009) was used. Due to the computational limitations, the smallest grid size was kept 1 m close to the walls of buildings. This grid size increased with the distance from the walls, using an expansion factor equal to 1.2. The domain included a total of 201354 cells and 37303 nodes for the west wind direction. For the winds from the north and south the domain has length, breadth and height as 491, 524 and 150 m, respectively. The number of cells and nodes remain same for all the domains. A mesh sensitivity analysis was made to verify the independence of the solution, following the COST 732 guidelines (COST, 2007), to confirm that the prediction result does not change significantly with different grid systems.

An Eulerian approach was applied for the simulation of 3D flow, assuming steady-state conditions. For the turbulence closure, a RNG k- ϵ model was used that calculated 3D fields of wind, turbulent viscosity, pressure and turbulence. For the PM₁₀ dispersion, a Lagrangian approach was used for the computation of the 3D concentration field. The dispersion model consists of a second phase of spherical particles in a Lagrangian frame of reference, dispersed in the continuous phase with coupling between the phases. The initial position, velocity and size of particles were introduced, and the stochastic tracking considered was the discrete random walk model. Atmospheric conditions were assumed as neutral. The RNG k- ϵ turbulence model was adopted that provided an analytical formula for turbulent Prandtl numbers. At the inlet, a logarithmic vertical wind profile was adopted; this assumed a reference velocity as 10 m s⁻¹ at 10 m height, based on the local measurement campaigns. The wind profile, turbulent kinetic energy, and turbulence dissipation rate was introduced as a user defined function (UDF) using the following formulation:

$$U_y = \frac{u^*}{\kappa} \ln \left(\frac{y + y_0}{y_0} \right) \quad (1)$$

where U_y (m s⁻¹) is the wind velocity at height, y ; κ (=0.42) is the Von Karman constant; y_0 (m) is the aerodynamic roughness length of the ground; u^* (m s⁻¹) is the friction velocity (Richards and Hoxey, 1993).

$$u^* = \frac{\kappa U_{10}}{\ln \left(\frac{10 + y_0}{y_0} \right)} \quad (2)$$

where U_{10} (m s⁻¹) is the wind velocity at 10 m height. The turbulent kinetic energy, ϵ (m² s⁻²), and turbulence dissipation rate, k (m² s⁻²), at the inlet is estimated using:

$$\epsilon = \frac{u_*^3}{\kappa(y + y_0)} \quad \text{and} \quad k = 3.33u_*^2 \quad (3)$$

The PM₁₀ emission rate in the street canyon was chosen as 1.82×10^{-6} kg s⁻¹. As described in Section 2.4, this source strength for local conditions was estimated using the ADMS–Urban model (CERC, 2006). Two line sources were added in the CFD domain, one for each lane, located at 0.1 m above the pavement level for simulating the height of the vehicles' exhaust pipe. A no-slip boundary condition was imposed at all solid surfaces i.e., the flow in the near-wall region was represented by the law-of-the-wall for mean velocity. A symmetry boundary was assumed at the top of the domain, assuming a zero flux of all the quantities across the horizontal plane.

2.3. The building configuration scenarios

Four building configuration scenarios were considered with the objective of studying the possibility of improvements in PM₁₀ concentrations within this street canyon (Fig. 3). The first configuration (Option 1) corresponds to the actual architectural layout on both sides of the street (see Fig. 3a). The remaining three configurations (Options 2, 3 and 4) consisted 'virtual' minor alterations in the arrangement of buildings on the south side of the street. For instance, Option 2 considers 4 m gaps between the buildings along the left hand, southern, side of the street (Fig. 3b). Option 3 considered 6 m wide gaps as opposed to 4 m assumed in 'Option 2' (Fig. 3c). The last configuration, Option 4, con-

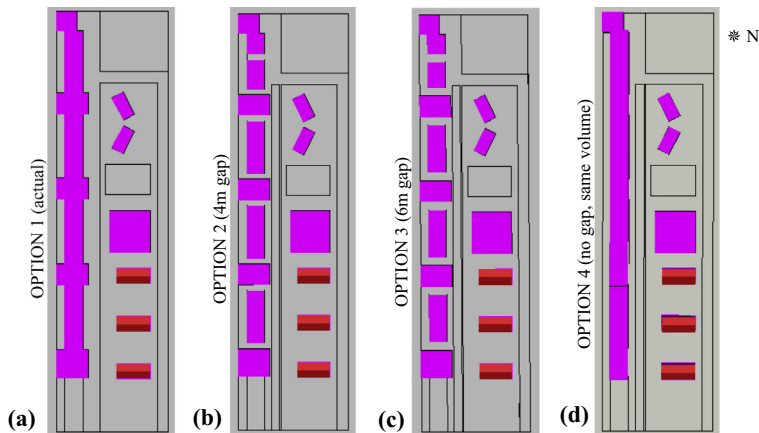


Fig. 3. The four building configuration scenarios considered for simulations: (a) the actual configuration (Option 1), (b) assuming 4 m gap between buildings (Option 2), (c) assuming 6 m gap between buildings (Option 3), and (d) assuming same volume and uniform geometry (Option 4).

sidered the equal volume of total buildings, as in Option 1, but assumed a uniform geometry having: (i) identical height (i.e. 20 m) on the both sides of building, and (ii) the same building width throughout (i.e. 261 m) the street, with no gap between the buildings (Fig. 3d).

2.4. Emissions characterisation

The main emission source in the selected domain is the traffic running on this road. PM_{10} emissions were calculated using ADMS-Urban model, considering the mean traffic number of vehicles in rush hours as the baseline scenario for the traffic emissions. The emission factors for traffic from ADMS-Urban for the year of 2010 were considered appropriate for this type of road in Portugal. The following inputs were provided to the model for emission estimates: total number of vehicles per hour in the street canyon, vehicle types (LDV, HDV, buses and motorcycle) and average vehicle speed (50 km h^{-1}), street width, canyon length, terrain type (urban), as well as average dimensions of the buildings. No other important sources of emissions were identified in the domain, so the only other values contributing for the PM_{10} concentration were the background concentrations. The background PM_{10} concentrations were considered as $20 \mu\text{g m}^{-3}$; these were adopted from the Portuguese Air Quality Station (Fidalguinhos station), which is classified as urban background station for this area.

2.5. Measurements of PM_{10} concentrations

PM_{10} concentrations were measured during a field campaign, performed at Avenida do Bocage street, from 17–20 October 2011 during the day time between 0900 and 1800 h (local time). The DustTrack model 8520 was used for the PM_{10} measurements. The sampler uses a suction pump to take the flow of 1.7 L min^{-1} through an optical chamber where the sample is backlit with a laser beam and the particles reflect this light that is read by a photo detector. The detection circuit converts the light into voltage that is proportional to the mass concentration of PM_{10} . Measurements were made at 7 different points that were 1.5 m above the ground level along the canyon length to gain the representative values. Fig. 4 shows the sampling locations. Summary of hourly average measured PM_{10} concentrations is provided in Table 1. Meteorological data was provided by the Instituto de Meteorologia. The average ambient temperature and relative humidity during the measurement campaigns were $25 \text{ }^\circ\text{C}$ and 40%, respectively. Predominant wind direction was noted as ‘west’ (i.e. along the street canyon).

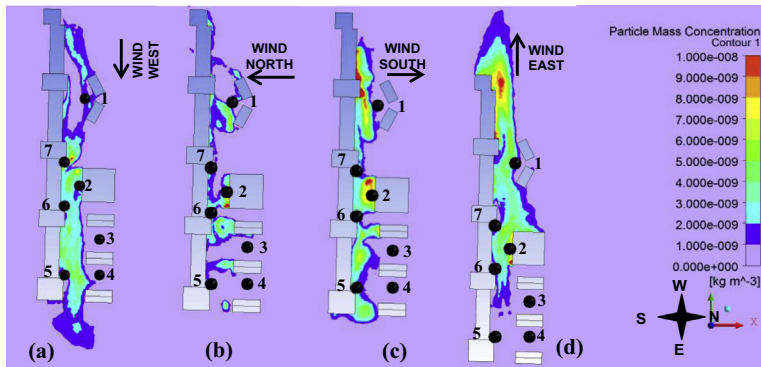


Fig. 4. Contour plots of PM_{10} concentrations at 1.5 m above the road level for the actual street configuration (i.e., Option 1) under the studied four main wind directions.

Table 1
 PM_{10} concentrations at 1.5 m high for Option 1 (actual configuration).

Designation	Location	PM_{10} Conc. ($\mu g m^{-3}$) west wind	PM_{10} Conc. ($\mu g m^{-3}$) north wind	PM_{10} Conc. ($\mu g m^{-3}$) south wind	PM_{10} Conc. ($\mu g m^{-3}$) east wind	PM_{10} measured Conc. ($\mu g m^{-3}$) west wind	WAC ($\mu g m^{-3}$)
Point 1	School	21.6	21.2	20.7	22.3	33.0	21.3
Point 2	Bingo	23.0	28.6	27.1	27.0	31.0	25.4
Point 3	Car park (border)	20.1	20.0	20.1	20.0	29.0	20.1
Point 4	Car park (middle)	20.4	20.0	20.1	20.0	29.0	20.2
Point 5	High building corner	20.5	20.6	22.7	20.0	27.0	20.9
Point 6	Residential building (east)	22.2	21.5	21.9	21.0	28.0	21.7
Point 7	Residential building (west)	25.0	20.9	22.5	20.7	28.0	22.8
Mean value	For the 7 points	21.8	21.8	22.1	21.6	29.3	21.8
Standard deviation	For the 7 points	1.75	3.04	2.66	2.53	2.06	1.85
Mean value	1.5 m plane (all domain)	20.8	20.5	21.0	21.1	–	20.8

3. Results and discussion

3.1. The base case

Fig. 4 shows the simulated results for PM_{10} concentrations for the actual street configuration (Option 1) under four different wind directions (west, north, south and east). The figure shows contour plots of PM_{10} concentrations at 1.5 m above the road level. This is a typical human breathing height for exposure (WHO, 2010). Only PM_{10} emissions from the traffic are considered for computations and no background concentrations are added in this case.

It is evident from the Fig. 4 that the highest values of PM_{10} concentrations are obtained for the conditions when the wind is coming from the south (cross canyon) and east (along canyon). The hot-spots (i.e. the locations with the highest concentrations) are appearing at the centre and at the end of the

street. In the case of winds from the south, this hot-spot appears as a result of the vortex induced by the relatively tall building located at the middle of the street. In the case of winds from the east, the hot-spot can be seen in the beginning of the street due to the limited dispersion of PM_{10} and at the end of the street due to the accumulation of the particle concentration along the street.

Table 1 shows the values of modelled PM_{10} concentrations at 1.5 m height above the road level, including both traffic and background contributions for 'Option 1'. Measured PM_{10} concentrations and the Weighted Average Concentrations (WAC) are also reported at all the 7 measurements points located in the street canyon (Fig. 4). The WAC is estimated using the Eq. (4) which is the mean concentration weighted by the wind direction frequency (f_i) i.e., the average number of times in each year, each of the four directions are observed. This allows evaluating the particle concentration for the whole year, considering all the different wind directions.

$$WAC = PM_{10} \times f_i \quad (4)$$

The highest modelled PM_{10} concentrations are found at Point 2 (Bingo building) with a value of $28.6 \mu\text{g m}^{-3}$ during the winds from the north. This point is located on the north end of the road near the largest building on this side, making difficult for the upstream wind to carry the pollutant outside the street. This point also shows one of the highest measured values. If we average the modelled PM_{10} concentrations over the all 7 points for each wind directions separately, the highest concentration ($22.1 \mu\text{g m}^{-3}$) comes out for southerly wind conditions. Considering the mean values at 1.5 m high plane, the highest measured value for easterly wind conditions was noted as $21.1 \mu\text{g m}^{-3}$. Modelled results in Table 1 show that the average concentrations varied modestly at sampling points, except a few showing larger differences. For instance, the highest and the lowest modelled concentrations are 28.6 and $20.0 \mu\text{g m}^{-3}$. They both are however below the daily mean and annual national limits for PM_{10} in Portugal, which are 50 and $40 \mu\text{g m}^{-3}$, respectively.

The WAC is important to study the weight of most frequent conditions. For example, the calculated value at point 1 is the 2nd highest for the easterly winds. However, when this value is weighed with the wind direction, the concentration values become the 4th highest. The differences in the WAC for average values across the street are not significant. However, comparison of individual points show important differences, indicating minimum and maximum values at Points 3 and 2 as 20.1 and $25.4 \mu\text{g m}^{-3}$, respectively.

Fig. 5 shows the measured and modelled concentrations of PM_{10} at 1.5 m above the road level. These values are reasonably close to each other but the CFD results show a slight under prediction at a few points 1 and 7. Point 1 and 7 are located near traffic lights and simulations does not take into account the start-stop or accelerating/decelerating speed conditions of vehicles – these could be the possible reasons for the increase in local PM_{10} emission rates and hence the difference in results.

3.2. PM_{10} concentrations in virtual configurations

Figs. 6–8 show the PM_{10} contour plots at 1.5 m above the road level due to traffic emissions (without the background) for the three virtual Options 1, 2 and 3, respectively. Each figure shows four sub-figures and each sub-figure represents the concentration contours for west, north, south, and east wind directions, respectively.

It is possible to observe from the Fig. 6 that north (Fig. 6b) and south (Fig. 6c) winds promote the best and the worst pollutant dispersion for this configuration. This configuration includes a 4 m wide gap between buildings, which has decreased the concentrations of PM_{10} in the street in comparison with the concentrations observed in real street canyon (Fig. 4). These gaps promote the wind flows through them and carry the emitted pollutants outside of the street. These findings are in accordance to those reported by Chan et al. (2003). They investigated the pollutant dispersion characteristics in a three-dimensional simulation of an urban street canyon for various building array geometries. They found that the cross-road introduces a horizontal path for the pollutants to disperse away, resulting in overall reduction in retention values, as compared with a continuous canyon.

Fig. 7 shows the PM_{10} contour plots for the 'Option 3' that assumes a 6 m wide gap between the buildings compared with 4 m wide gap in 'Option 2'. Comparison of Figs. 6 and 7 show similar distributions of PM_{10} concentrations. However some local differences can appear due to different air flow

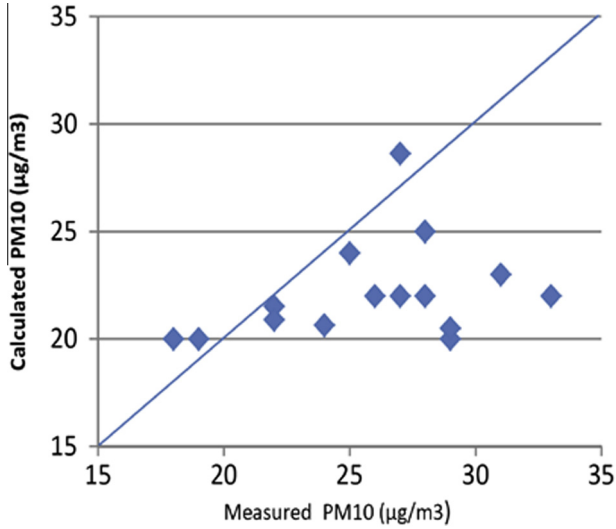


Fig. 5. Measured vs. modelled PM₁₀ concentrations at points 1 to 7.

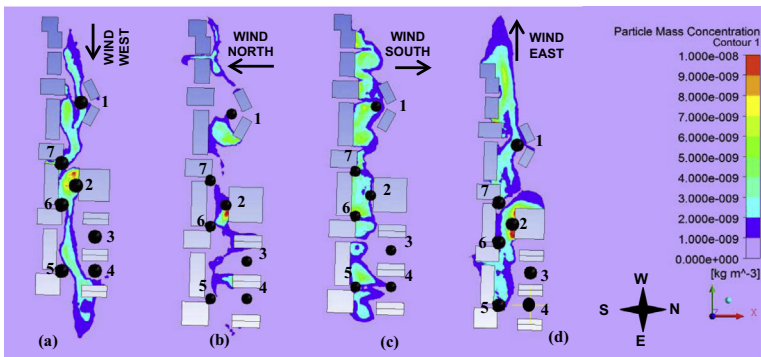


Fig. 6. Contour plots of PM₁₀ concentrations at 1.5 m above the road level for the Option 2 under the wind directions.

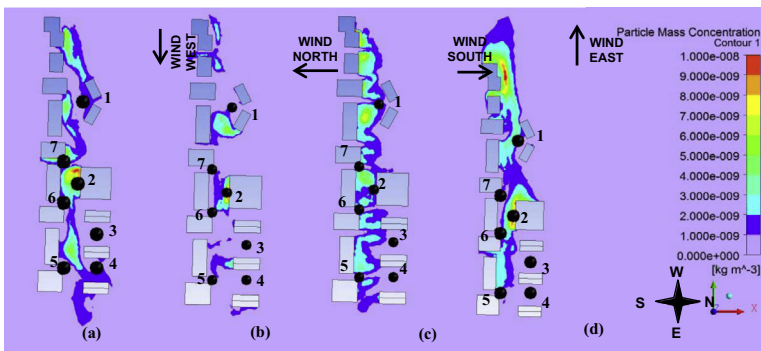


Fig. 7. Contour plots of PM₁₀ concentrations at 1.5 m above the road level for the 'Option 3' under the four wind directions.

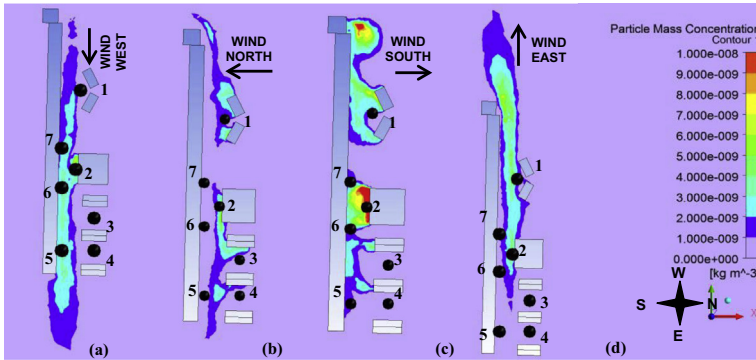


Fig. 8. Contour plots of PM_{10} concentrations at 1.5 m above the road level for the Option 4 under the four main wind directions.

Table 2

PM_{10} concentrations at 1.5 m above the road level for Options 1, 2, 3 and 4.

Designation	PM_{10} Conc. ($\mu\text{g}/\text{m}^3$) west wind				PM_{10} Conc. ($\mu\text{g}/\text{m}^3$) north wind				PM_{10} Conc. ($\mu\text{g}/\text{m}^3$) south wind				PM_{10} Conc. ($\mu\text{g}/\text{m}^3$) east wind			
	1	2	3	4	1	2	3	4	1	2	3	4	1	2	3	4
Point 1	21.6	22.3	20.9	20.0	21.2	20.8	20.8	21.3	20.7	22.7	21.0	21.5	22.3	22.2	21.2	22.0
Point 2	23.0	25.7	25.9	24.1	28.6	23.2	26.8	22.8	27.1	21.8	21.1	30.7	27.0	27.6	26.8	23.0
Point 3	20.1	20.0	20.0	20.0	20.0	20.0	20.0	20.1	20.1	20.0	20.3	20.0	20.0	20.0	20.0	20.0
Point 4	20.4	20.0	20.4	20.0	20.0	20.0	20.0	20.2	20.1	20.7	20.5	20.6	20.0	20.0	20.0	20.0
Point 5	20.5	20.0	20.0	23.2	20.6	20.0	20.0	20.4	22.7	20.4	20.1	21.1	20.0	21.2	20.1	20.1
Point 6	22.2	21.0	20.1	23.3	21.5	20.1	20.1	20.0	21.9	23.9	20.2	21.9	21.0	20.7	20.5	20.4
Point 7	25.0	23.3	22.9	22.2	20.9	20.0	22.9	22.2	22.5	21.2	20.0	21.4	20.7	20.0	20.1	20.7
Mean value (1.5 m plane)	20.8	20.6	20.6	20.4	20.5	20.4	20.4	20.4	21.0	20.6	20.6	20.8	21.1	20.9	20.9	20.6

acceleration through the gaps (Table 2). This means that small differences in the gap size does not produce significant differences in the average PM_{10} concentration, but can cause significant local differences due the local eddies. These eddies, in general, allow higher particle dispersion but these can increase the retention time at some points, particularly for easterly wind. This effect can be observed in the Figs. 6 and 7 on the side of downwind building for easterly winds.

By looking at the Fig. 8 (Option 4), it is possible to observe that for along-canyon wind directions, the dispersion of PM_{10} is promoted when all buildings have the same side cross width, allowing a good sweep by the wind in the street (Table 2).

Results in Table 2 for Option 4 show that at hot spot point 2, PM_{10} concentrations decay from $30.8 \mu\text{g m}^{-3}$ for south (cross-canyon) wind to $23.0 \mu\text{g m}^{-3}$ for east (along-canyon) due to channelling of flow, representing $\sim 23\%$ lower PM_{10} concentrations. For the same hot spot point 2, under south (cross-canyon) wind, the PM_{10} concentrations decay from $27.1 \mu\text{g m}^{-3}$ (Option A) to $21.8 \mu\text{g m}^{-3}$ (Option B) and $21.1 \mu\text{g m}^{-3}$ (Option C) due to the introduction of gaps between buildings, representing a particle dilution of $\sim 20\%$ and $\sim 22\%$ for Options 2 and 3, respectively, compared with the Option 1.

3.3. Comparison of PM_{10} mean concentrations obtained from different configurations

The results of mean value of PM_{10} concentrations for a horizontal plane located at 1.5 m above the road level show that the configuration with different buildings size and no gap between them (option 1) generated the worst case having many points with increased concentrations (see Fig. 5 and Table 2). The implementation of gaps between buildings (options 2 and 3) promotes wind circulation crossing the street, improving pollutant removal for southerly (cross-canyon) wind directions (see Figs. 5–7

and 12). There is also an improvement in pollutant removal, mainly in areas with local recirculation near the gaps, compared with Option 1. Buildings with the same height (Option 4) seem to be a good configuration for along-canyon wind direction, since no local recirculation is promoted (Fig. 8).

For cross canyon wind directions, 'Option 4' shows a slight improvement in PM_{10} concentrations compared with 'Option 1' (Table 2). Comparison of Option 4 under southerly winds with Options 2 and 3 shows a slight increase of PM_{10} concentration, mainly because the air flow crossing the street is not promoted locally (Table 2). Chan et al. (2003) refers that urban variations in building height and breadth and intricate roof level configurations promote ventilation. Our results are in line with their findings that the combination of a uniform geometry in one side of the street with intricate geometry in the other side (Option 4) is the preferable solution for all wind direction, when mean values are considered (Table 2). The improvement in PM_{10} concentrations is modest for the cross-canyon winds and these findings are in agreement with the conclusions drawn by Chan et al. (2003).

Analysis of the different sampling points individually indicates the point 2 as a location with higher PM_{10} concentration (Table 2). It is possible to see that the highest values appear for the Options 1 and 4 under southerly winds (Fig. 9). This is because the downwind building has lower height compared with the upwind building that results in two set of vortex (i.e., main and secondary). The secondary vortex is responsible for the increase in PM_{10} concentrations near the downwind building wall (see Fig. 9a and c). For the northerly winds, the upwind building has the lowest building height and the air flow promotes the pollutant dispersion in this case (Fig. 10). In Option 1, the effect of southerly wind direction is not noticed at point 2, because the buildings on both side of the street have the same height. This effect of building heights on pollutant dispersion is in accordance with the findings of Assimakopoulou et al. (2003). In Options 2 and 3, the difference in building height at point 2 is reduced, but the gaps promote lateral flows at the same time which reduces the pollutant concentration for southerly winds. This effect continues to be present during the northerly winds in comparison with Option 1, but the gaps do not produce any favourable effect when compared with Option 4 (Fig. 11). At the point 2 in Option 1, the different height of the buildings are on the side of the road that promotes three-dimensional effect on the air flow, which can only be observed by the 3D simulations (see Figs. 11 and 12).

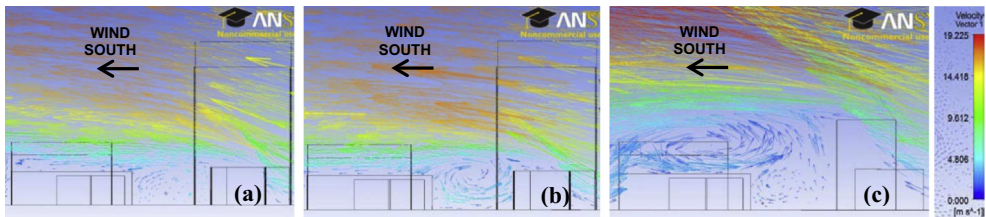


Fig. 9. Vertical plan of wind velocity vectors for south wind direction on point 2 for: (a) Option 1, (b) Option 3, and (c) Option 4.

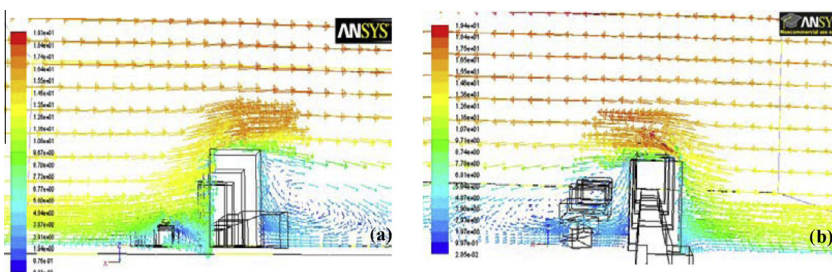


Fig. 10. Wind velocity vectors for south wind direction (a) and north wind direction (b) on point 2 for 'Option 1'.

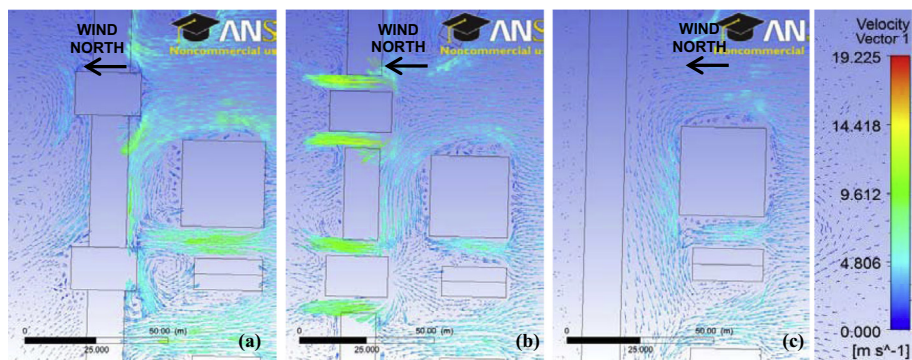


Fig. 11. Horizontal plan of wind velocity vectors for north wind direction: (a) Option 1, (b) Option 3, (c) Option 4.

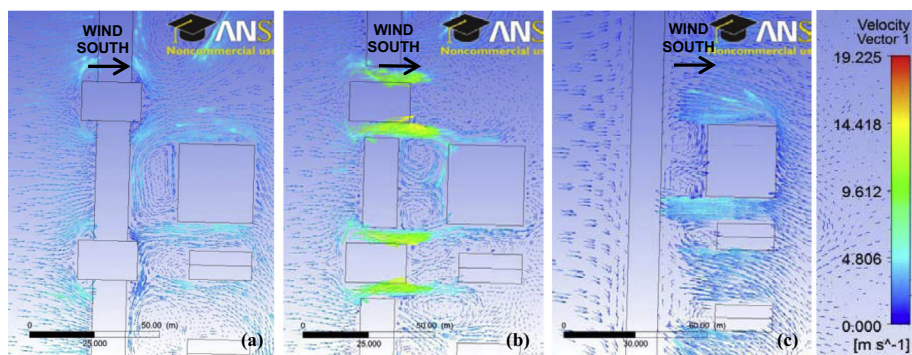


Fig. 12. Horizontal plan of wind velocity vectors for south wind direction: (a) Option 1, (b) Option 3, and (c) Option 4.

Table 3

The WAC values for Options 1, 2, 3 and 4 for all hot spots.

Designation	Location	Option 1	Option 2	Option 3	Option 4
Point 1	School	21.3	21.8	20.8	20.8
Point 2	Bingo	25.4	24.1	24.9	24.7
Point 3	Car park (border)	20.1	20.0	20.1	20.0
Point 4	Car park (middle)	20.2	20.1	20.3	20.0
Point 5	High building corner	20.9	20.2	20.1	21.6
Point 6	Residential building (east)	21.7	21.2	21.2	21.8
Point 7	Residential building (west)	22.8	21.6	21.2	21.3
Mean value	1.5 m plane (all domain)	20.8	20.5	20.6	20.4

Table 3 shows the computed values of the WAC at 1.5 m above the road for the four different configurations chosen in this study. Generally, the results show better concentration values for Option 4 while the Option 1 presents the worst case. The WAC for PM_{10} values varies from $20.8 \mu g m^{-3}$ in the actual configuration (i.e., Option 1) to $20.4 \mu g m^{-3}$ for Option 4. The variation of WAC mean value for the horizontal plane is not very significant. However considering specific points showing the hot-spots, the location with the highest reduction (7%) is point 7, showing a decrease from $22.8 \mu g m^{-3}$ for Option 1 to $21.2 \mu g m^{-3}$ for Option 2.

4. Summary and conclusions

The CFD code FLUENT was used to simulate the dispersion of PM₁₀ in a busy street canyon in Barreiro city, Portugal. Four different configurations of the street canyon, including the real street and three virtual scenarios after modifying the real street configurations are studied. The aims were to investigate the influence of changes in building configurations on the concentration levels of PM₁₀ at various selected points located at a breathing height (i.e. 1.5 m). The results indicate that changes in street configurations and building geometries have influenced the PM₁₀ concentrations in the studied street canyon. It is also possible to reduce PM₁₀ concentrations, and hence improve the air quality in a street canyon, after certain alterations in the street configurations. Irrespective of street configurations, wind direction also plays a dominant role in the variation of PM₁₀ concentrations. In general, the best average concentrations levels were observed for winds from the west and east (along canyon) directions for uniform geometry (Option 4). The formation of vortices at the corners of buildings was found to promote the trapping of pollutants at pedestrian level while the uniform buildings geometry with least corners helped in avoiding such formations. Gaps between the buildings (Options 2 and 3) during the cross-canyon winds, showed improved PM₁₀ concentrations. For specific hot spots under cross-canyon wind conditions, PM₁₀ concentrations decay ~20% and ~22% for Options 2 and 3 compared with Option 1, due to the introduction of gaps between buildings. Interestingly, when mean PM₁₀ concentrations values are considered for all the planes located at 1.5 m above the road level, no significant improvements were noted with 6 m wider gaps between buildings compared with only 4 m gaps for the same wind directions. For along-canyon winds, buildings with uniform dimensions helped in avoiding some local trapping of pollutants at pedestrian level. Results show that for specific hot spots, PM₁₀ concentrations decay ~23% due to the channelling of flow, compared with those observed during the cross-canyon wind direction. The use of WAC was found to be a good measure to assess the influence of canyon configuration, because it takes into account the frequency of different wind directions. The findings of this work suggest that the building configuration plays an important role in PM concentrations in street canyons.

Acknowledgements

The authors also wish to acknowledge the support from the Comissão de Coordenação e Desenvolvimento Regional de Lisboa e Vale do Tejo (CCDR-LVT) and Instituto de Meteorologia for the meteorological data provided.

References

- Amorim, J.H., Lopes, M., Borrego, C., Tavares, R., Miranda, A.I., 2010. Air quality modelling as a tool for sustainable urban traffic management. In: Proceedings from the 18th International Conference on Modelling, Monitoring and Management of Air Pollution, WIT Transactions on Ecology and the Environment, vol. 136, pp. 3–14.
- Ansys, 2009. ANSYS Fluent 12.0, Getting Started Guide. Fluent Guides.
- Assimakopoulou, V.D., ApSimon, H.M., Moussiopoulos, N., 2003. A numerical study of atmospheric pollutant dispersion in different two-dimensional street canyon configurations. *Atmospheric Environment* 37, 4037–4049.
- Awasthi, S., Chaudhry, K.K., 2009. Numerical simulation and wind tunnel studies of pollution dispersion in an isolated street canyon. *International Journal of Environment and Waste Management* 4, 243–255.
- Britter, R.E., Hanna, S.R., 2003. Flow and dispersion in urban areas. *Annual Review of Fluid Mechanics* 35, 469–496.
- CERC, 2006. ADMS-Urban, an urban air quality management system. User guide -version 2.2 Cambridge, UK.
- Chan, A.T., Au, W.T.W., So, E.S.P., 2003. Strategic guidelines for street canyon geometry to achieve sustainable street air quality – part II: multiple canopies and canyons. *Atmospheric Environment* 37, 2761–2772.
- COST, 2007. Best practice guideline for the CFD simulation of flows in the urban environment, Quality assurance and improvement of microscale meteorological models, COST action 732. ISBN 3-00-018312-4.
- De Paul, F.T., Sheih, C.M., 1986. A tracer study of dispersion in an urban street canyon. *Atmospheric Environment* 20, 455–459.
- Di Sabatino, S., Buccolieri, S., Pulvirenti, B., Britter, R., 2008. Flow and pollutant dispersion in street canyons using FLUENT and ADMS-Urban. *Environmental Modelling and Assessment* 13, 369–381.
- EEA, 2011. Air quality in Europe – 2011 report, European Environment Agency.
- Ehrhard, J., Khatib, I.A., Winkler, C., Kunz, R., Moussiopoulos, N., Ernst, G., 2000. The microscale model MIMO: development and assessment. *Journal of Wind Engineering and Industrial Aerodynamics* 85, 163–176.
- Garcia, J., Coelho, L., Gouveia, C., Cerdeira, R., Louro, C., Ferreira, T., Baptista, M., 2010. Analysis of human exposure to urban air quality in a children population. *International Journal of Environment and Pollution* 40, 94–108.
- Heal, M.R., Kumar, P., Harrison, R.M., 2012. Particles, air quality, policy and health. *Chemical Society Reviews* 41, 6606–6630.

- Holmes, N.S., Morawska, L., 2006. A review of dispersion modelling and its application to the dispersion of particles: an overview of different dispersion models available. *Atmospheric Environment* 40, 5902–5928.
- Kumar, P., Morawska, L., 2013. Energy-pollution nexus for urban buildings. *Environmental Science & Technology* 47, 7591–7592.
- Kumar, P., Fennell, P., Langley, D., Britter, R., 2008. Pseudo-simultaneous measurements for the vertical variation of coarse, fine and ultra fine particles in an urban street canyon. *Atmospheric Environment* 42, 4304–4319.
- Kumar, P., Garmory, A., Ketzel, M., Berkowicz, R., Britter, R., 2009. Comparative study of measured and modelled number concentrations of nanoparticles in an urban street canyon. *Atmospheric Environment* 43, 949–958.
- Kumar, P., Gurjar, B.R., Nagpure, A., Harrison, R.M., 2011a. Preliminary estimates of nanoparticle number emissions from road vehicles in megacity Delhi and associated health impacts. *Environmental Science and Technology* 45, 5514–5521.
- Kumar, P., Ketzel, M., Vardoulakis, S., Pirjola, L., Britter, R., 2011b. Dynamics and dispersion modelling of nanoparticles from road traffic in the urban atmospheric environment – a review. *Journal of Aerosol Science* 42, 580–603.
- Kumar, P., Robins, A., Vardoulakis, S., Britter, R., 2010. A review of the characteristics of nanoparticles in the urban atmosphere and the prospects for developing regulatory controls. *Atmospheric Environment* 44, 5035–5052.
- Martins, A., Cerqueira, M., Ferreira, F., Borrego, C., Amorim, J.H., 2009. Lisbon air quality: evaluating traffic hot-spots. *International Journal Environment and Pollution* 39, 306–320.
- Mochida, A., Lizuka, S., Tominaga, Y., Yu-Fat Lun, I., 2011. Up-scaling CWE models to include mesoscale meteorological influences. *Journal of Wind Engineering and Industrial Aerodynamics* 99, 187–198.
- Nikolova, I., Janssen, S., Vos, P., Vrancken, K., Mishra, V., Berghmans, P., 2011. Dispersion modelling of traffic induced ultrafine particles in a street canyon in Antwerp, Belgium and comparison with observations. *Science of the Total Environment* 412, 243–336.
- Pospisl, J., Jicha, M., 2008. Determination of the PM10 urban threshold velocity of resuspension in an inner part of urban area. *Croatian Meteorological Journal* 43, 657–661.
- Richards, P.J., Hoxey, R.P., 1993. Appropriate boundary conditions for computational wind engineering models using the k- ϵ turbulence model. *Journal of Wind Engineering and Industrial Aerodynamics* 46, 145–153.
- Sagrado, A., Beeck, J., Rambaud, P., Olivari, D., 2002. Numerical and experimental modelling of pollutant dispersion inside a street canyon. *Journal of Wind Engineering and Industrial Aerodynamics* 90, 321–339.
- Santiago, J.L., Martín, F., 2008. SLP-2D: a new Lagrangian particle model to simulate pollutant dispersion in street canyons. *Atmospheric Environment* 42, 3927–3936.
- Schlunzen et al., 1996. Hints for Using the Mesoscale Model METRAS. Technical Report 6, Meteorologisches Institut der Universität Hamburg.
- Vardoulakis, S., Fisher, B.E.A., Pericleous, K., Gonzalez-Flesca, N., 2003. Modelling air quality in street canyons: a review. *Atmospheric Environment* 37, 155–182.
- Wang, P., Mu, H., 2010. Numerical simulation of pollutant flow and dispersion in different street layouts. *International Journal of Environmental Studies* 67, 155–167.
- WHO, 2004. Outdoor air pollution: assessing the environment burden of disease at national and local levels.
- WHO, 2010. WHO guidelines for indoor air quality: selected pollutants.
- Zhou, Y., Levy, J., 2008. The impact of urban street canyons on population exposure to traffic-related primary pollutants. *Atmospheric Environment* 42, 3087–3098.